Anal Bioanal Chem (2016) 408:7321–7327
DOI 10.1007/s00216-016-9608-7

RESEARCH PAPER

Label-free electrochemical genosensor based on mesoporous silica thin film

Maroua Saadaoui[1] · Iñigo Fernández[2] · Gema Luna[2] · Paula Díez[2] · Susana Campuzano[2] · Noureddine Raouafi[1] · Alfredo Sánchez[2] · José M. Pingarrón[2] · Reynaldo Villalonga[2]

Received: 8 March 2016 / Revised: 25 April 2016 / Accepted: 28 April 2016 / Published online: 28 May 2016

Abstract A novel label-free electrochemical strategy for nucleic acid detection was developed by using gold electrodes coated with mesoporous silica thin films as sensing interface. The biosensing approach relies on the covalent attachment of a capture DNA probe on the surface of the silica nanopores and further hybridization with its complementary target oligonucleotide sequence, causing a diffusion hindering of an $Fe(CN)_6^{3-/4-}$ electrochemical probe through the nanochannels of the mesoporous film. This DNA-mesoporous silica thin film-modified electrodes allowed sensitive (91.7 A/M) and rapid (45 min) detection of low nanomolar levels of synthetic target DNA (25 fmol) and were successfully employed to quantify the endogenous content of *Escherichia coli* 16S ribosomal RNA (rRNA) directly in raw bacterial lysate samples without isolation or purification steps. Moreover, the 1-month stability demonstrated by these biosensing devices enables their advanced preparation and storage, as desired for practical real-life applications.

Keywords Genosensor · Mesoporous silica film · Cyclic voltammetry · *E. coli* · 16S rRNA · DNA

Published in the topical collection *Chemical Sensing Systems* with guest editors Maria Careri, Marco Giannetto, and Renato Seeber.

Maroua Saadaoui and Iñigo Fernández contributed equally to this work.

Electronic supplementary material The online version of this article (doi:10.1007/s00216-016-9608-7) contains supplementary material, which is available to authorized users.

✉ Alfredo Sánchez
alfredosanchez@quim.ucm.es

✉ José M. Pingarrón
pingarro@quim.ucm.es

✉ Reynaldo Villalonga
rvillalonga@quim.ucm.es

[1] Department of Chemistry, Faculty of Sciences, University of Tunis El Manar, Rue Béchir Salem Belkheria, Tunis El-Manar, 2092 Tunis, Tunisia

[2] Department of Analytical Chemistry, Faculty of Chemistry, Complutense University of Madrid, 28040 Madrid, Spain

Introduction

Genosensor technology has demonstrated to be a powerful tool for clinical diagnosis, biomedical research, food quality assurance, and environmental monitoring [1, 2]. For this reason, the design of original, simple, and cost-effective analytical methods for the sensitive and accurate detection and quantification of specific nucleic acid sequences through hybridization mechanisms constitutes a main research topic in bioanalytical chemistry.

During last decades, a great variety of genosensors have been developed by using electrochemical, optical, calorimetric, and piezoelectric transduction strategies [3–6]. Although optical systems have been the most widely employed, electrochemical methods have great prospective due to the simplicity, easy preparation, relative low cost, and possibility to be miniaturized in portable point-of-care devices [7].

The assembly of original genosensors has been largely benefited by the use of novel nanomaterials and nanohybrids as advanced transducer elements. In this sense, a large number of electrochemical genosensors with improved analytical properties has been developed by using carbon nanotubes [8], graphene [9], metal and metal oxide nanoparticles [10–12], and other nanomaterials as constituents of the sensing interface. In general, these electrochemical genosensors involve the use of organic and metalorganic redox indicators [13, 14], enzymes [15, 16], or nanoparticles [17] as labeling

elements. However, such labeling strategies imply tedious and relative complex detection protocols, which limit the further application of these genosensors in portable, patient-oriented, and patient-operated point-of-care devices [18].

In this context, mesoporous silica thin films offer relevant advantages for the assembly of affinity-based electrochemical biosensors [19]. These nanomaterials have large surface area-to-volume ratio and a large content of hydroxyl groups at the surface, favoring easy modification with silane-coupling reagents. Growing of mesoporous silica films with perpendicular pores on electrode surface provides a unique array of nanochannels with excellent permeability properties [20, 21]. These nanopores can be rationally tuned by chemical transformation at the outer or inner surface, allowing modification of the specific properties of film electrodes, such as charge, selective permeability, hydrophobicity/hydrophilicity, and electrocatalysis [19, 22]. Selective immobilization of biomacromolecules with affinity properties can also confer biomolecular recognition properties to these nanomaterials. In addition, mesoporous silica films are rigid inorganic matrix with high mechanical stability, allowing designing of stable biosensor devices.

Recently, we reported the use of mesoporous silica thin films as electrochemical transduction elements for the assembly of a DNAzyme-based sensor for ascorbic acid and Cu(II) [23], as well as a sensor system for transglutaminase activity quantification [24]. The rational of these devices relied on the effects of the biorecognition process on the diffusion ability of an electrochemical probe through the nanochannels of the mesoporous film. Following this general sensing concept, and as proof-of-concept that such diffusion-controlled mechanism can be extended to nucleic acid detection, we report herein the assembly of an original electrochemical genosensor using gold electrodes coated with DNA-modified mesoporous silica thin films. The behavior of this novel scaffold was evaluated with a synthetic target DNA and its applicability successfully demonstrated for the direct determination of the target *Escherichia coli* 16S ribosomal RNA (rRNA) gene in raw lysate solutions in only 45 min.

Materials and methods

Reagents and apparatus

All reagents and synthetic DNA oligonucleotides were acquired from Sigma-Aldrich (USA). The sequences of the nucleic acids were as follows:

- Capture probe sequence, end-group modified with a heptylamine-phosphoramidite moiety: 5′-[AmC7F] CTT CCT CCC CGC TGA-3′. This probe was designed to be fully complementary to both synthetic DNA and the partial region of the *E. coli* 16S rRNA targets [25].
- Synthetic target DNA sequence: 5′-TCA GCG GGG AGG AAC GGA GTA AAG TTA ATA-3′. This sequence is a copy of partial region of the *E. coli* 16S rRNA gene (position 432–461 according to the 5′→3′ nucleotide sequence) [25].
- Double-base mismatch sequence: 5′-T**A**A GCG GGG AGG A**G**C GGA GTA AAG TTA ATA-3′.

All these oligonucleotides were dissolved in nuclease free water at 100 μM final concentration, aliquoted into smaller volumes, and stored at −20 °C.

A FRA2 μAutolab type III potentiostat/galvanostat was used for all electrochemical experiments. A three-electrode system was employed, by using a gold disk (2.0 mm diameter) modified with the functionalized mesoporous silica thin film as working electrode. In addition, an Ag/AgCl/KCl (3 M) and a Pt wire were employed as reference and counter electrodes, respectively. High-resolution transmission electron microscopy (HRTEM) measurements were performed with a JEOL JEM-2100 microscope. Atomic force microscopy (AFM) studies were performed with a SPM Nanoscope III microscope. Field emission scanning electron microscopy (FE-SEM) measurements were carried out by using a JEOL JSM 7600F microscope.

Assembly of the DNA-functionalized nanostructured electrode

Mesoporous silica thin films were deposited under potentiostatic conditions on Au electrodes according to the method reported by Walcarius and co-workers [20] with some modifications. Briefly, a sol mixture consisting of 4.4 mmol tetraethyl orthosilicate, 20 mL ethanol (95 %), 20 mL of 0.1 M $NaNO_3$ aqueous solution, 1 mM HCl, and 1.4 mmol cetyltrimethylammonium bromide was prepared under magnetic stirring. The sol was aged for 2.5 h under stirring before use. The Au electrode was then immersed in the precursor solution and electrodeposition was achieved under quiescent conditions by applying a cathodic potential of −1.3 V vs Ag/AgCl during 15 s. The electrode was then removed and rinsed with water to avoid deposition of nanoparticulated structures. The film-coated electrode was then dried and aged overnight in an oven at 130 °C. To modify the outer surface of the film, the electrode was dipped into a 50 mM methyltriethoxysilane (MTES) solution in toluene and kept under stirring at room temperature during 1 h. The electrode was then exhaustively washed with a methanol solution containing 0.1 M HCl under moderate stirring for 15 min. To functionalize the inner surface of the pores, the electrode was further dipped into an ethanolic solution containing 2.26 mmol of (3-glycidyloxypropyl) trimethoxysilane (GPTMS) for 1 h. The electrode was further washed with double-distilled water, and then

10 μL of 1.0 μM solution of the capture DNA probe in the working buffer (100 mM sodium phosphate buffer, pH 7.8) was dropped onto the electrode surface. After 45 min incubation at 4 °C, the electrode was washed with the working buffer and kept at 4 °C in buffer solution until use.

Voltammetric detection of DNA hybridization

Hybridization assay was performed by dropping 10 μL of the hybridization solution containing the target DNA on the surface of the modified electrode. The DNA hybridization was carried out at 4 °C during 45 min. The electrode was then thoroughly rinsed with working buffer solution and cyclic voltammograms were recorded in 0.1 M KCl solution containing 5 mM $K_3[Fe(CN)_6]/K_4[Fe(CN)_6]$ (1:1).

The analytical signal used to monitor hybridization corresponded to the difference between the current measured from the cyclic voltammograms at +350 mV recorded in the absence and in the presence of the target DNA sequence.

Isolation of 16S rRNA samples [29]

One milliliter of *E. coli* (CCT 515, 10^9 CFU/mL) suspension was centrifuged at 10,000 rpm during 10 min, and the resulting pellet was then suspended in 10 μL of 1 M NaOH solution in ultrapure water. After 5 min incubation, the solution was 100-fold diluted in the working buffer to provide the 16S rRNA genetic material for voltammetric determination.

Results and discussion

Figure 1 shows the strategy on which the assembly of the label-free DNA biosensor was based. In a first step, gold electrode surface was coated with a mesoporous silica thin film by electrodeposition of a sol precursor solution containing tetraethyl orthosilicate as film-forming compound and cetyltrimethylammonium bromide as porogenic agent [22].

Through this electrodeposition process, Au surface was provided with a suitable non-conductive mineral scaffold for the assembly of the DNA biosensor via covalent immobilization of the capture DNA probe. In addition, this film provided the electrode with an array of well-ordered nanometric pores suitable to act as channels enabling the diffusion of an electroactive probe to the sensing surface.

The formation of the mesoporous silica thin film on the gold electrode surface was confirmed by different microscopic and spectroscopic techniques, as is illustrated in Fig. S1 in the electronic supplementary material (ESM). AFM studies revealed a film planar structure, with few nanoparticulated adducts deposited on its surface (Fig. S1A in the ESM). The average thinness of the mesoporous film was estimated as 43 nm in agreement with that previously reported [23, 24]. FE-SEM analysis also confirmed the 2D planar structure of the silica film (Fig. S1B in the ESM) as well as the presence of a few number of silica nanoparticles. As can be observed by HR-TEM, the electrodeposited film exhibited a homogenous array of uniform and vertically aligned nanochannels of c.a. 2.5 nm diameter, arranged in a honeycomb structure (Fig. S1C in the ESM). The typical hexagonal symmetry of mesoporous silica as confirmed by selected area electron diffraction analysis (SAED), as can be observed in the inset of Fig. 2c. In addition, the composition of the film was confirmed by energy dispersive spectroscopy (Fig. S1D in the ESM).

The assembly of the label-free electrochemical genosensor implied coating of the film planar surface with hydrophobic methyl moieties by treatment with MTES in toluene. This treatment was performed before releasing the porogenic surfactant from the pores, to preserve the active SiO_2 surface at the inner nanochannels. However, we cannot discard that this treatment could lead to some surfactant molecules leaching in solution, allowing further partial modification of the inner surface of the pore with MTES. Modification with MTES aims to avoid further immobilization of the capture DNA so far from the nanopores and also to avoid unspecific adsorption of the target nucleic acids chains on the film. This unspecific adsorption could cause additional blocking of nanopores not related to the hybridization process, as can be observed in Fig. S2 (ESM). The film was further washed with HCl in methanol to release the surfactant from the pores, allowing further activation of their inner area with reactive epoxy groups by treatment with GPTMS. Thereafter, capture DNA probe was covalently immobilized on the electrode surface by reaction of the active epoxy groups at the mesoporous film with the primary amino group at the 5′-end residue of the nucleic acid molecule.

Cyclic voltammetry was employed to monitor the changes occurring at the electrode surface during the assembly of the electrochemical genosensor. Figure 2 shows the voltamograms recorded at the different electrode architectures using $[Fe(CN)_6]^{4-/3-}$ as redox probe. Electrodeposition of the mesoporous silica thin film provoked, as expected, a noticeable interfacial change on the Au surface leading to the disappearance of the voltammetric response at the modified electrode (curve b). This fact suggests full coverage of the electrode surface by the mesoporous film filled with the surfactant molecules. Similar pattern was observed after modification with MTES (data not show). Further washing with ethanolic HCl allows removal of the surfactant molecules from the nanopores. This removal process was confirmed by the appearance of voltammetric peaks in the cyclic voltammogram (curve c), due to the diffusion of the $[Fe(CN)_6]^{4-/3-}$ ions to the electrode surface through the open nanopores. Functionalization of mesoporous thin film with GPTMS (curve d) and further immobilization of the capture DNA probe (curve e) caused steric hindrance to the diffusion of the redox probe to the gold

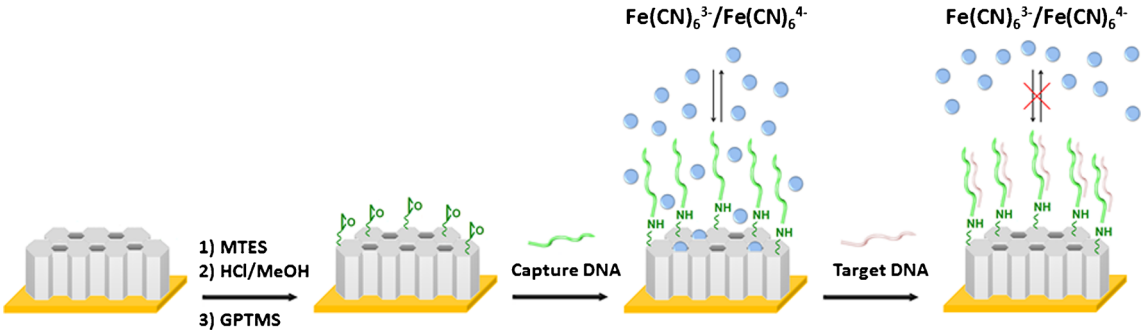

Fig. 1 Schematic display of the processes involved in the assembly of the label-free electrochemical DNA biosensor

electrode surface through the nanopores. This fact was confirmed by the progressive decrease of the redox peaks in the respective voltammograms.

Similar conclusions could be deduced from electrochemical impedance spectroscopy (EIS) measurements as it is illustrated in Fig. 3. All experimental data were fitted to a conventional Randles equivalent circuit. Electrodeposition of the surfactant-templated film caused a significant increase in the electron transfer resistance after Au surface modification (see inset in Fig. 3), thus confirming a high coverage of the electrode surface with the surfactant-templated film, avoiding the diffusion of the $[Fe(CN)_6]^{4-/3-}$ ions to the electrode interface. Further modification with MTES provided similar EIS pattern (data not show). A significant decrease in the semicircle diameter of the Nyquist plot was observed after removal of the surfactant from the nanopores. This confirmed the expected decrease in the electron transfer resistance at the interface as a consequence of the surfactant molecule release from the nanopores, thus allowing diffusion of the redox probe to the gold electrode surface. Subsequent functionalization of the sensor surface with GPTMS and capture DNA strand caused a progressive increase in the electron transfer resistance, suggesting proper silanization and immobilization of the DNA molecules on the mesoporous film.

The behavior of the DNA-modified electrode toward a complementary DNA sequence was evaluated by cyclic voltammetry using $[Fe(CN)_6]^{4-/3-}$ ions as electroactive probe. As can be observed in Fig. 4, a noticeable decrease in the voltammetric peaks was observed upon incubation of the electrode with the complementary target DNA, suggesting successful hybridization on the genosensor surface. Such hybridization should provoke steric hindrance at the entrance of the nanopores, limiting the diffusion of the redox probe to the electrode surface. A linear relationship between the decrease in the oxidation peak current and the target DNA concentration suggested that the constructed biosensor could be employed for analytical purposes.

In order to optimize the assembly conditions for the genosensor, the influence of different working variables on the analytic response of the DNA-modified electrode toward 100 nM target DNA was tested (Fig. S3 in the ESM). In this sense, the analytical signal ($/\Delta i/$) was established as the absolute value of the difference in the current intensity of the oxidation peaks in the voltammograms recorded with the capture DNA-modified electrode before and after hybridization with the target DNA. Larger differences in peak currents were

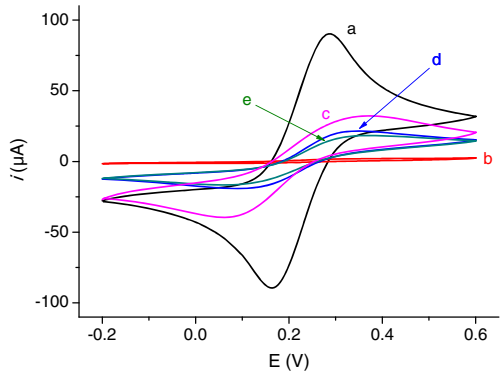

Fig. 2 Cyclic voltammograms recorded at the Au electrode in 0.1 M KCl solution containing 5 mM $K_3[Fe(CN)_6]/K_4[Fe(CN)_6]$ (1:1) before (*a*) and after electrodeposition of the mesoporous silica thin film (*b*), washing with ethanolic HCl (*c*), modification with GPTMS (*d*), and immobilization of the capture DNA (*e*). Scan rate, 50 mV/s

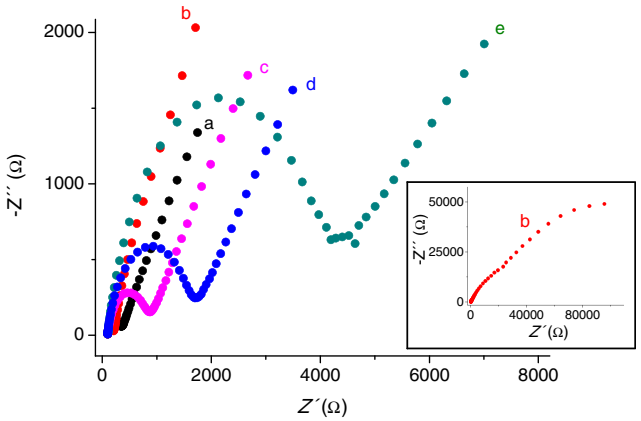

Fig. 3 Nyquist plots recorded at the Au electrode in 0.1 M KCl solution containing 5 mM $K_3[Fe(CN)_6]/K_4[Fe(CN)_6]$ (1:1) before (*a*) and after electrodeposition of the mesoporous silica thin film (*b*), washing with HCl/EtOH (*c*), modification with GPTMS (*d*), and immobilization of the capture DNA probe (*e*)

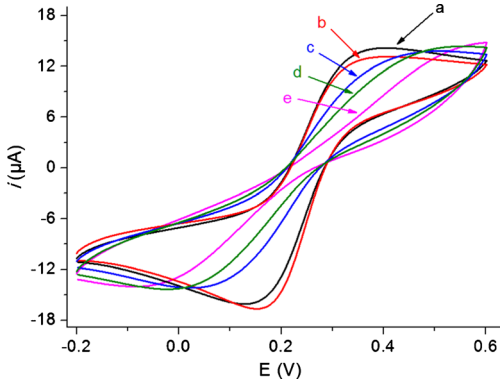

Fig. 4 Cyclic voltammograms recorded with the DNA-modified electrode in 0.1 M KCl solution containing 5 mM $K_3[Fe(CN)_6]/K_4[Fe(CN)_6]$ (1:1) before (*a*) and after incubation with 20 nM (*b*), 40 nM (*c*), 60 nM (*d*), and 100 nM (*e*) synthetic target DNA. Scan rate, 50 mV/s

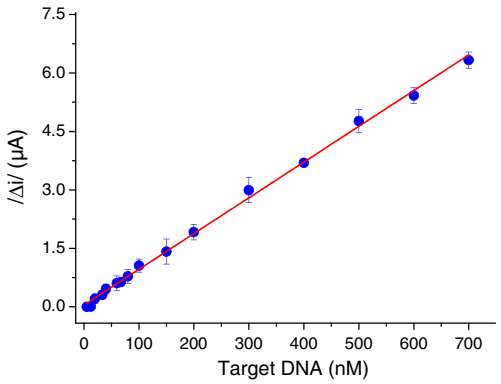

Fig. 5 Calibration plot obtained for the determination of the synthetic target DNA. *Error bars* were estimated as triple of the standard deviation ($n = 3$)

achieved by incubating the electrodes with 10 pmol of capture DNA during 45 min.

Moreover, the effect of the hybridization time was also checked. As it can be seen in Fig. S4A (ESM), larger currents were recorded after incubation of the electrode with complementary DNA for 45 min or longer, and accordingly, this incubation time was employed for further hybridization experiments. In addition, high difference in the current intensity of the oxidation peaks was obtained by measure at +350 mV (Fig. S4B in the ESM), and this potential value was used for further analytical determination.

Under these optimal conditions, the genosensor showed excellent electroanalytical performance for the label-free determination of complementary DNA. Figure 5 shows the calibration curve obtained for this genosensor, which showed a wide linear range from 5 to 700 nM ($r = 0.995$, $n = 6$), according to the following equation:

$$|\Delta i|(A) = 91.7 \times C_{DNA}(M) + 4 \times 10^{-7}$$

The limit of detection for the genosensor was determined to be 2.5 nM which, considering the sample volume required per analysis (10 μL), corresponded to a detectable absolute amount of less than 25 fmol of the synthetic target DNA. This LOD value was calculated according to the $3S_b/m$ criterion, where m is the slope of the calibration curve and S_b was estimated as the standard deviation of six different cyclic voltammetry signals recorded for the lowest target DNA concentration measured. Although other electrochemical DNA biosensors have recently reported similar or lower limits of detection for DNA hybridization, they commonly involve more complex electrode architectures and labeling strategies [26–28]. In addition, the label-free genosensor reported here showed a very high sensitivity of 91.7 A/M.

It is well known that cyclic voltammetry is less sensitive than other electroanalytical techniques, such as EIS. However, cyclic voltammetry is highly reproducible and was enough to achieve a low detection limit and high sensitivity as demonstrated. On the other hand, voltamperometric techniques require less complex and less expensive hardware architecture to construct miniaturized and portable biosensors for nucleic acid detection, which is at the end, one of the main goals of our research.

The selectivity of the label-free DNA biosensor was examined by challenging the system with a two-based mismatched synthetic DNA sequence. As can be seen in Fig. S5 (ESM), the two-base-mismatched DNA, even in a ten times higher concentration, yielded a lower decrease in the voltammetric signal (voltammogram c) compared to that observed for the fully complementary sequence (voltammogram b), reflecting only a partial duplex formation with the double mismatched sequence. These results revealed that the developed label-free electrochemical DNA biosensor can be successfully employed to detect the target nucleic acid sequence with high selectivity.

The reproducibility of the measurements made with different sensors prepared in the same manner was evaluated by measuring the voltammetric responses for 100 nM synthetic target DNA. The relative standard deviation (RSD) value calculated from the measurements carried out with six different sensors was 7.4 %, demonstrating a great reproducibility of the whole sensor fabrication and the signal transduction protocols. In addition, it was observed that modified electrodes retained more than 93 % of the sensitivity to determine 100 nM of the synthetic target DNA sequence after 1 month of storage at 4 °C in the working buffer (Fig. S6 in the ESM). This attractive stability performance promises the convenient usage of pre-prepared electrodes after prolonged time storage without any treatment.

The practical utility of this new biodetection platform was tested for the detection of the endogenous 16S rRNA content in a raw *E. coli* lysate prepared following the protocol reported previously by Wu et al. [29]. As it is displayed in Fig. 6, the voltammetric signal obtained from this raw bacterial lysate sample (voltammogram b) can be clearly distinguished from that observed without the bacterial rRNA target (voltammogram a).

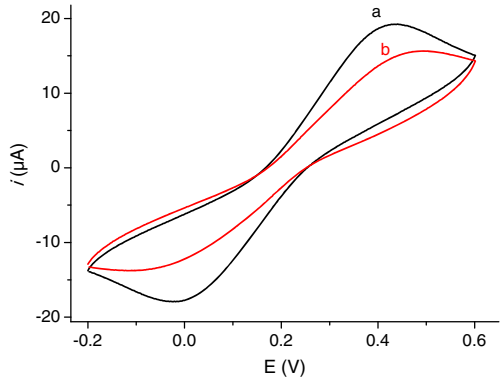

Fig. 6 Cyclic voltammograms recorded with the DNA-modified electrode in 0.1 M KCl solution containing 5 mM $K_3[Fe(CN)_6]/K_4[Fe(CN)_6]$ (1:1) before (*a*) and after incubation with the raw bacterial lysate target solution (*b*). Scan rate, 50 mV/s

An average concentration of 42 nM 16S rRNA was estimated for this *E. coli* extract by interpolation of the voltammetric response into the calibration curve obtained with the synthetic target DNA (Fig. 5).

Taking into account the 16S rRNA content in the bacteria (2×10^4 copies/cell) [29], the concentration of *E. coli* in the initial sample was estimated to be 1.3×10^9 cell/mL, in agreement with those determined by conventional cell count analysis (10^9 CFU/mL). These results demonstrated the applicability of this new sensing platform to detect directly raw bacterial rRNA without isolation or purification steps, allowing pathogen determination in only 45 min.

Conclusions

In this work, we described a simple, cost-effective, label-free approach for the selective and one-pot voltammetric detection of nucleic acids in only 45 min, based on the DNA hybridization-controlled diffusion of an electrochemical probe through the nanochannel at a gold electrode coated with a mesoporous silica thin film. The good performance of this new platform, illustrated both for the sensitive determination of synthetic target DNA and raw bacterial rRNA, and its attractive 1-month storage stability, indicated its great potential for real-world applications. This strategy can be extended to many other genosensor architectures or bioaffinity assays, and can be easily miniaturized to develop point-of-care electrochemical devices for a wide range of nucleic acid testing, including biomedical diagnostics, food safety, biothreat detection, and forensic analysis.

Acknowledgments The financial support from the Spanish Ministry of Economy and Competitiveness CTQ2014-58989-P, CTQ2011-24355, CTQ2015-71936-REDT, CTQ2015-64402-C2-1-R and Comunidad de Madrid S2013/MIT-3029, Programme NANOAVANSENS is gratefully acknowledged. M.S. thanks the University of Tunis El-Manar for "the Alternance Bourse" grant.

Compliance with ethical standards

Conflict of interest The authors declare that they have no conflict of interest.

References

1. Vidal JC, Bonel L, Ezquerra A, Hernández S, Bertolín JR, Cubel C, et al. Electrochemical affinity biosensors for detection of mycotoxins: a review. Biosens Bioelectron. 2013;49:146–58.
2. Kirsch J, Siltanen C, Zhou Q, Revzin A, Simonian A. Biosensor technology: recent advances in threat agent detection and medicine. Chem Soc Rev. 2013;42:8733–68.
3. Zhao WW, Xu JJ, Chen HY. Photoelectrochemical DNA biosensors. Chem Rev. 2014;114:7421–41.
4. Hamidi-Asl E, Palchetti I, Hasheminejad E, Mascini M. A review on the electrochemical biosensors for determination of microRNAs. Talanta. 2013;115:74–83.
5. Hu R, Liu T, Zhang XB, Huan SY, Wu C, Fu T, et al. Multicolor fluorescent biosensor for multiplexed detection of DNA. Anal Chem. 2014;86:5009–16.
6. Kim S, Choi SJ. A lipid-based method for the preparation of a piezoelectric DNA biosensor. Anal Biochem. 2014;458:1–3.
7. Liu A, Wang K, Weng S, Lei Y, Lin L, Chen W, et al. Development of electrochemical DNA biosensors. Trends Anal Chem. 2012;37:101–11.
8. Benvidi A, Rajabzadeh N, Mazloum-Ardakani M, Heidari MM. Comparison of impedimetric detection of DNA hybridization on chemically and electrochemically functionalized multi-wall carbon nanotubes modified electrode. Sensors Actuators B Chem. 2015;207:673–82.
9. Li B, Pan G, Avent ND, Lowry RB, Madgett TE, Waines PL. Graphene electrode modified with electrochemically reduced graphene oxide for label-free DNA detection. Biosens Bioelectron. 2015;72:313–9.
10. Yola ML, Eren T, Atar N. A novel and sensitive electrochemical DNA biosensor based on Fe@ Au nanoparticles decorated graphene oxide. Electrochim Acta. 2014;125:38–47.
11. Huang KJ, Liu YJ, Wang HB, Wang YY. A sensitive electrochemical DNA biosensor based on silver nanoparticles-polydopamine@graphene composite. Electrochim Acta. 2014;118:130–7.
12. Wang J, Shi A, Fang X, Han X, Zhang Y. An ultrasensitive supersandwich electrochemical DNA biosensor based on gold nanoparticles decorated reduced graphene oxide. Anal Biochem. 2015;469:71–5.
13. Gebala M, La Mantia F, Schuhmann W. Kinetic and thermodynamic hysteresis imposed by intercalation of proflavine in ferrocene-modified double-stranded DNA. ChemPhysChem. 2013;14:2208–16.
14. Yang Z, d'Auriac MA, Goggins S, Kasprzyk-Hordern B, Thomas KV, Frost CG, et al. A novel DNA biosensor using a ferrocenyl intercalator applied to the potential detection of human population biomarkers in wastewater. Environ Sci Technol. 2015;49:5609–17.
15. Cao X. Ultra-sensitive electrochemical DNA biosensor based on signal amplification using gold nanoparticles modified with molybdenum disulfide, graphene and horseradish peroxidase. Microchim Acta. 2014;181:1133–41.
16. Liu L, Xiang G, Jiang D, Du C, Liu C, Huang W, et al. Electrochemical gene sensor for mycoplasma pneumoniae DNA using dual signal amplification via a Pt@Pd nanowire and horseradish peroxidase. Microchim Acta. 2016;183:379–87.
17. Wu L, Xiong E, Zhang X, Zhang X, Chen J. Nanomaterials as signal amplification elements in DNA-based electrochemical sensing. Nano Today. 2014;9:197–211.
18. Ahmed MU, Saaem I, Wu PC, Brown AS. Personalized diagnostics and biosensors: a review of the biology and technology needed for personalized medicine. Crit Rev Biotechnol. 2014;34:180–96.

19. Walcarius A, Kuhn A. Ordered porous thin films in electrochemical analysis. Trends Anal Chem. 2008;27:593–603.
20. Walcarius A, Sibottier E, Etienne M, Ghanbaja J. Electrochemically assisted self-assembly of mesoporous silica thin films. Nat Mater. 2007;6:602–8.
21. Kao KC, Lin CH, Chen TY, Liu YH, Mou CY. A general method for growing large area mesoporous silica thin films on flat substrates with perpendicular nanochannels. J Am Chem Soc. 2015;137:3779–82.
22. Mousty C, Walcarius A. Electrochemically assisted deposition by local pH tuning: a versatile tool to generate ordered mesoporous silica thin films and layered double hydroxide materials. J Solid State Electrochem. 2015;19:1905–31.
23. Saadaoui M, Fernández I, Sánchez A, Díez P, Campuzano S, Raouafi N, et al. Mesoporous silica thin film mechanized with a DNAzyme-based molecular switch for electrochemical biosensing. Electrochem Commun. 2015;58:57–61.
24. Fernández I, Sánchez A, Díez P, Martínez-Ruiz P, Di Pierro P, Porta R, et al. Nanochannel-based electrochemical assay for transglutaminase activity. Chem Commun. 2014;87:13356–8.
25. Liao JC, Mastali M, Gau V, Suchard MA, Møller AK, Bruckner DA, et al. Use of electrochemical DNA biosensors for rapid molecular identification of uropathogens in clinical urine specimens. J Clin Microbiol. 2006;44:561–70.
26. Miao P, Wang B, Meng F, Yin J, Tang Y. Ultrasensitive detection of microRNA through rolling circle amplification on a DNA tetrahedron decorated electrode. Bioconjug Chem. 2015;26:602–7.
27. Zhang Y, Geng X, Ai J, Gao Q, Qi H, Zhang C. Signal amplification detection of DNA using a sensor fabricated by one-step covalent immobilization of amino-terminated probe DNA onto the polydopamine-modified screen-printed carbon electrode. Sensors Actuators B Chem. 2015;221:1535–41.
28. Qian Y, Wang C, Gao F. Ultrasensitive electrochemical detection of DNA based on Zn 2+ assistant DNA recycling followed with hybridization chain reaction dual amplification. Biosens Bioelectron. 2015;63:425–31.
29. Wu J, Balasubramanian S, Kagan D, Manesh KM, Campuzano S, Wang J. Motion-based DNA detection using catalytic nanomotors. Nat Commun. 2010;1:36.